Anibare Bay

Chapter 8
Nauru

The contributions of Andrew Kaierua, Russ Kun, Franklin Teimitsi and Douglas Audoa from the Department of Commerce, Industry and Environment are gratefully acknowledged

Introduction

This chapter provides a brief description of Nauru, its past and present climate as well as projections for the future. The climate observation network and the availability of atmospheric and oceanic data records are outlined. The annual mean climate, seasonal cycles and the influences of large-scale climate features such as the South Pacific Convergence Zone and patterns of climate variability (e.g. the El Niño-Southern Oscillation) are analysed and discussed. Observed trends and analysis of rainfall, extreme events, sea-surface temperature, ocean acidification, mean and extreme sea levels are presented. Projections for air and sea-surface temperature, rainfall, sea level, ocean acidification and extreme events for the 21st century are provided. These projections are presented along with confidence levels based on expert judgement by Pacific Climate Change Science Program (PCCSP) scientists. The chapter concludes with a summary table of projections (Table 8.3). Important background information including an explanation of methods and models is provided in Chapter 1. For definitions of other terms refer to the Glossary.

8.1 Climate Summary

8.1.1 Current Climate

- Air temperatures in Nauru are fairly constant throughout the year and are closely related to sea-surface temperatures.
- The wet season usually starts in November and continues to April of the next calendar year. Drier conditions occur during the months of May to October.
- Rainfall in Nauru is affected by both the Intertropical Convergence Zone, and the South Pacific Convergence Zone.
- Annual and seasonal rainfall trends for Nauru for the period 1950–2009 are not statistically significant.
- The main influence on interannual climate variability in Nauru is the El Niño-Southern Oscillation.
- The sea-level rise near Nauru measured by satellite altimeters since 1993 is about 5 mm per year.
- The main climate extreme experienced by Nauru is drought, which can last as long as three years. Nauru does not experience tropical cyclones.

8.1.2 Future Climate

Over the course of the 21st century:

- Surface air temperature and sea-surface temperature are projected to continue to increase (*very high* confidence).
- Annual and seasonal mean rainfall is projected to increase (*high* confidence).
- The intensity and frequency of days of extreme heat are projected to increase (*very high* confidence).
- The intensity and frequency of days of extreme rainfall are projected to increase (*high* confidence).
- The incidence of drought is projected to decrease (*moderate* confidence).
- Ocean acidification is projected to continue (*very high* confidence).
- Mean sea-level rise is projected to continue (*very high* confidence).

8.2 Country Description

Located just south of the equator in the western South Pacific Ocean, Nauru lies at approximately 0.5°S and 167°E. It is a raised atoll with an area of 21 km^2. Approximately 6 km long (NE-SW) and 4 km wide (NW-SE), Nauru has a maximum elevation of 71 m. The island has been mined extensively in the past for phosphate. The Exclusive Economic Zone has an area of 320 000 km^2. There is no official capital but the Yaren District is the largest settlement and where the Government offices are located (Nauru's First National Communication under the UNFCCC, 1999; Nauru's Pacific Adaptation to Climate Change, 2006). The estimated population in 2010 was 9976 (Nauru Country Statistics, SOPAC, 2010).

The main economic sector was the mining and export of phosphate, which is now virtually exhausted. Few other resources exist and most necessities are imported from Australia. There is only small scale subsistence agriculture (Nauru's National Committee on Climate Change, 1999; PACC, 2005).

Figure 8.1: Island of Nauru

8.3 Data Availability

Historical climate data exist for several stations in Nauru, and have been merged into a single station composite. Meteorological observations were initially conducted by the British Phosphate Corporation then later taken at the old wireless radio station and Nauru Airport. Currently observations are taken by an automatic weather station near Yaren. Data are available here from 1893 to present for rainfall and 1951 to present for air temperature, however there are significant gaps in the air temperature record. Rainfall data from 1950 to 2009 have been used. This record is homogeneous and more than 99% complete. There are insufficient air temperature data from 1950 to 2009 for air temperature trend analyses. The search for historical hard copy and digitised climate data for Nauru is ongoing.

Monthly-averaged sea-level data are available from the 1970s (1974–1994 and 1993–present). A global positioning system instrument to estimate vertical land motion was deployed at Nauru in 2003 and will provide valuable direct estimates of local vertical land motion in future years. Both satellite (from 1993) and in situ sea-level data (1950–2009; termed reconstructed sea level; Volume 1, Section 2.2.2.2) are available on a global 1° x 1° grid.

Long-term locally-monitored sea-surface temperature data are unavailable for Nauru, so large-scale gridded sea-surface temperature datasets have been used (HadISST, HadSST2, ERSST and Kaplan Extended SST V2; Volume 1, Table 2.3).

8.4 Seasonal Cycles

Nauru has consistent monthly mean air temperatures throughout the year (Figure 8.2). Its air temperatures are closely related to the sea-surface temperatures, which also are fairly constant throughout the year.

The wet season usually starts in November and continues to April of the next calendar year. Drier conditions occur during the months of May to October. Both the Intertropical Convergence Zone (ITCZ), which sits to the north of Nauru for most of the year, and the South Pacific Convergence Zone (SPCZ), which sits to the south, bring rainfall to Nauru. The higher rainfall in the wet seasons is caused by the ITCZ moving south and the SPCZ strengthening and expanding north at that time of year.

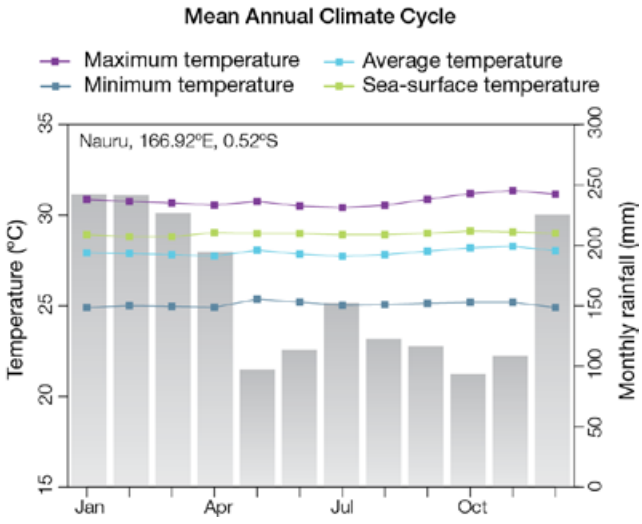

Figure 8.2: Mean annual cycle of rainfall (grey bars) and daily maximum, minimum and mean air temperatures at Nauru, and local sea-surface temperatures derived from the HadISST dataset (Volume 1, Table 2.3). Average air temperatures are calculated from 1951–1980, average rainfall and sea-surface temperatures from 1961–1990.

8.5 Climate Variability

As described earlier, gaps in the climate record of Nauru prevent the calculation of up-to-date trends. There is, however, sufficient historical data to determine rainfall variability.

The annual rainfall of Nauru has extremely high variability (standard deviation is 1151 mm) and the main influence on this climate variability is the El Niño-Southern Oscillation (ENSO) (Table 8.1). During El Niño years, Nauru is warmer and usually much wetter than average, receiving up to 4500 mm of rainfall. La Niña years are associated with a delayed onset of the wet season and drier than normal conditions, often resulting in an extended drought. In some La Niña years, Nauru only receives around 500 mm of rainfall.

Table 8.1: Correlation coefficients between indices of key large-scale patterns of climate variability and minimum and maximum temperatures (Tmin and Tmax) and rainfall at Nauru. Only correlation coefficients that are statistically significant at the 95% level are shown.

Climate feature/index		Dry season (May-October)			Wet season (November-April)		
		Tmin	Tmax	Rain	Tmin	Tmax	Rain
ENSO	Niño3.4			0.76			0.66
	Southern Oscillation Index			-0.77		0.46	-0.62
Interdecadal Pacific Oscillation Index							
ENSO Modoki Index			0.41	0.25			0.66
Number of years of data		29	29	60	28	27	63

Weather station maintenance, Tropical Western Pacific Climate Research Station

8.6 Observed Trends

8.6.1 Air Temperature

Due to incomplete historical air temperature records, observed air temperature trends for Nauru for the period 1950–2009 are unable to be calculated.

8.6.2 Rainfall

Annual and seasonal rainfall trends for Nauru for the period 1950–2009 are not statistically significant (Figure 8.3).

Table 8.2: Annual and seasonal trends in rainfall at Nauru for the period 1950–2009. Asterisks indicate significance at the 95% level. Persistence is taken into account in the assessment of significance as in Power and Kociuba (in press).

	Nauru Rain (mm per 10 yrs)
Annual	+11
Wet season	-37
Dry season	+38

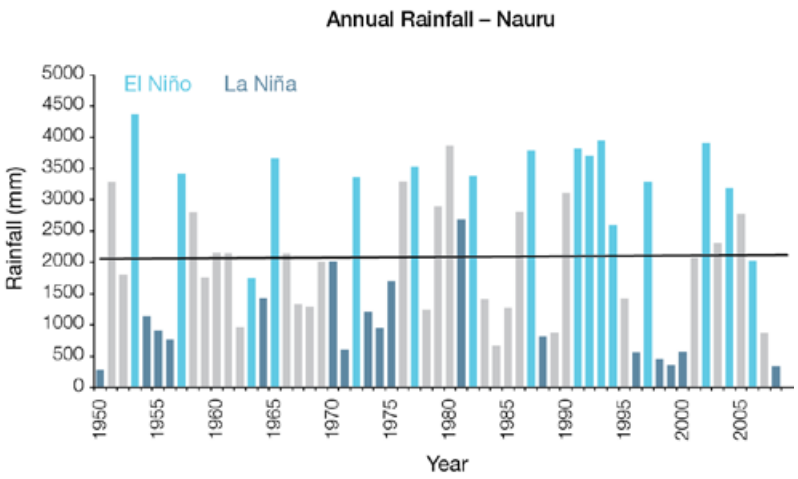

Figure 8.3: Annual rainfall at Nauru. Light blue, dark blue and grey bars denote El Niño, La Niña and neutral years respectively.

8.6.3 Extreme Events

Being so close to the equator, Nauru does not experience tropical cyclones. The main climate extreme experienced by Nauru is drought, which can last as long as three years. Droughts occur when La Niña events decrease the surrounding sea-surface temperature, resulting in less cloud and rainfall. Prolonged droughts cause a lowering of the underground freshwater lens, resulting in water supply problems and severe stress on natural systems.

8.6.4 Sea-Surface Temperature

Water temperatures around Nauru have risen gradually since the 1950s. Since the 1970s the rate of warming has been approximately 0.12°C per decade. Figure 8.6 shows the 1950–2000 sea-surface temperature changes (relative to a reference year of 1990) from three different large-scale sea-surface temperature gridded datasets (HadSST2, ERSST and Kaplan Extended SST V2; Volume 1, Table 2.3). At these regional scales, natural variability may play a large role in the sea-surface temperature trends making it difficult to identify any long-term trends.

8.6.5 Ocean Acidification

Based the large-scale distribution of coral reefs across the Pacific and the seawater chemistry, Guinotte et al. (2003) suggested that seawater aragonite saturation states above 4 were optimal for coral growth and for the development of healthy reef ecosystems, with values from 3.5 to 4 adequate for coral growth, and values between 3 and 3.5, marginal. Coral reef ecosystems were not found at seawater aragonite saturation states below 3 and these conditions were classified as extremely marginal for supporting coral growth.

In the Nauru region, the aragonite saturation state has declined from about 4.5 in the late 18th century to an observed value of about 3.9 ± 0.1 by 2000.

8.6.6 Sea Level

Monthly averages of the historical tide gauge, satellite (since 1993) and gridded sea-level (since 1950) data agree well after 1993 and indicate interannual variability in sea levels of about 23 cm (estimated 5–95% range) after removal of the seasonal cycle (Figure 8.8). The sea-level rise near Nauru measured by satellite altimeters (Figure 8.4) since 1993 is about 5 mm per year, slightly larger than the global average of 3.2 ± 0.4 mm per year. This rise is partly linked to a pattern related to climate variability from year to year and decade to decade (Figure 8.8).

8.6.7 Extreme Sea-Level Events

The annual climatology of the highest daily sea levels has been evaluated from hourly tide gauge measurements at Nauru (Figure 8.5). High tides show relatively small variation throughout the year maximising in December and January. There is no variation in the seasonal component of sea level, possibly due to Nauru's nearly equatorial position (0.5°S). The short-term component varies throughout the year and tends to indicate the occurrence of extreme water levels from November to March with distinct peaks centred on March and December. Consistent with this the top 10 sea-level events in the record all occur from November to March. The La Niña years are associated with near average sea levels from January to July and lower sea levels from July to December. On the other hand the short-term water levels tend to be higher during El Niño years and this is reflected in the top 10 sea-level events for which the majority occurred in El Niño or ENSO-neutral years.

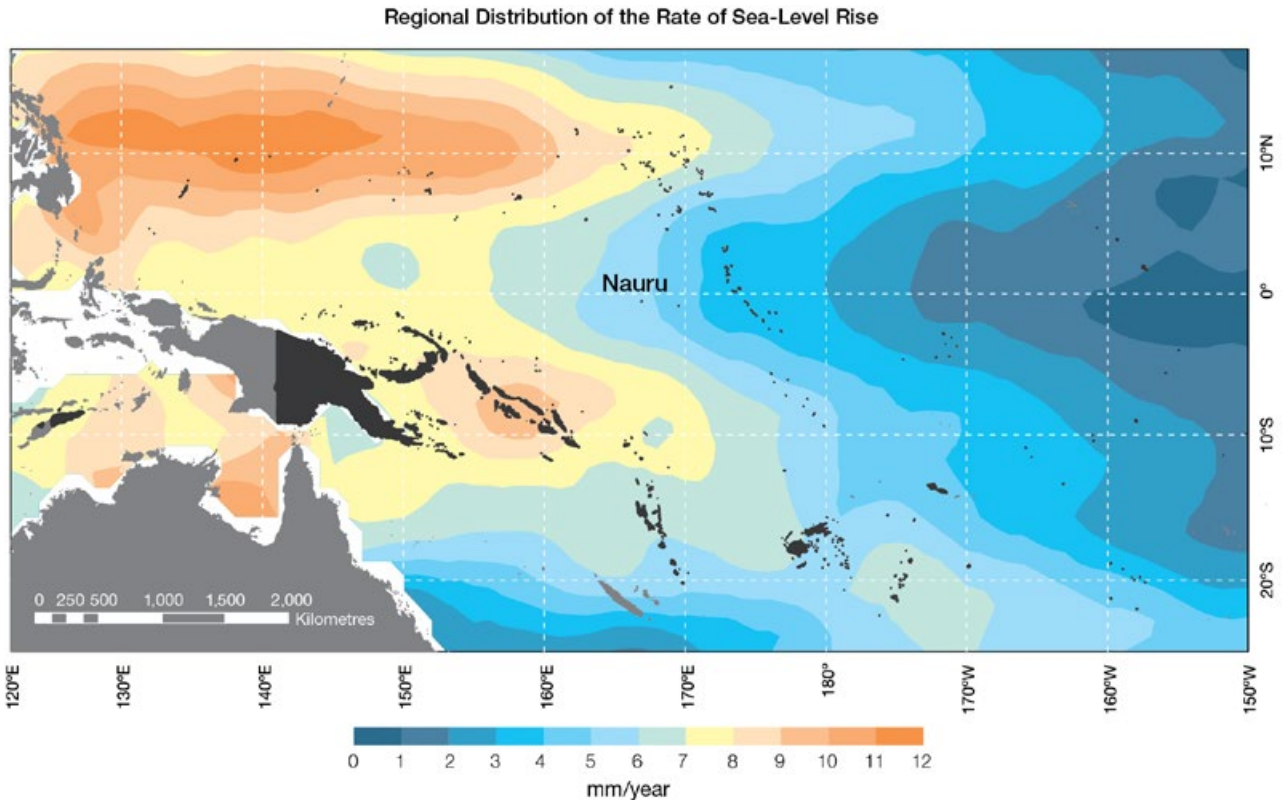

Figure 8.4: The regional distribution of the rate of sea-level rise measured by satellite altimeters from January 1993 to December 2010, with the location of Nauru indicated. Further detail about the regional distribution of sea-level rise is provided in Volume 1, Section 3.6.3.2.

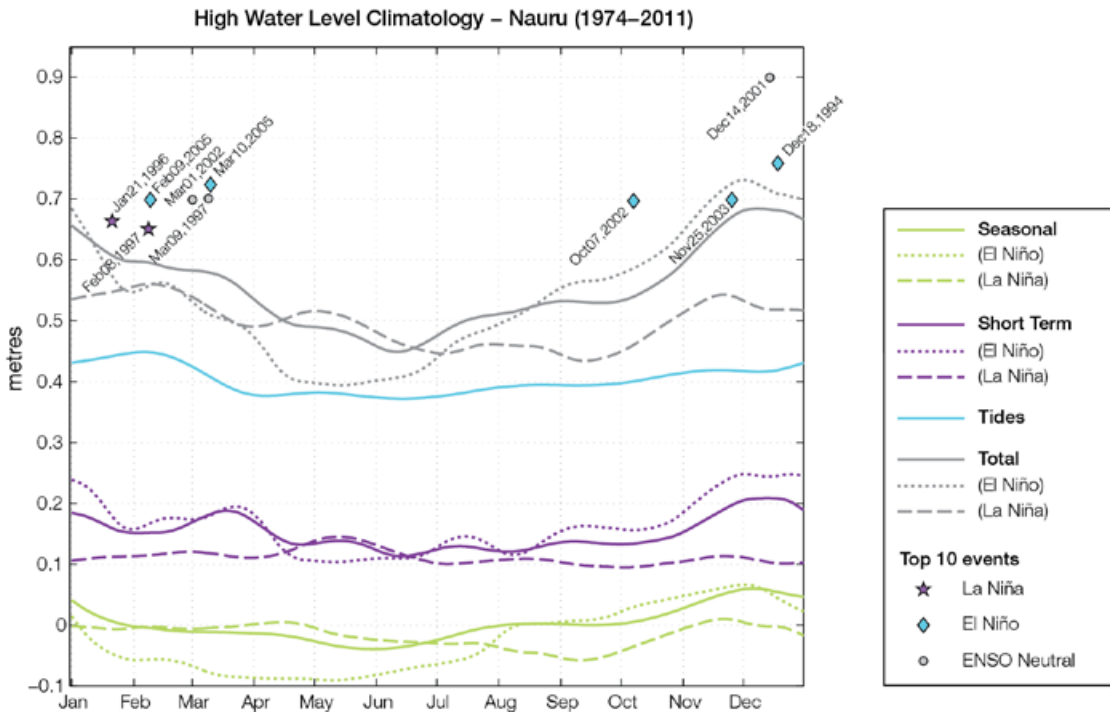

Figure 8.5: The annual cycle of high waters relative to Mean Higher High Water (MHW) due to tides, short-term fluctuations (most likely associated with storms) and seasonal variations for Nauru. The tides and short-term fluctuations are respectively the 95% exceedence levels of the astronomical high tides relative to MHHW and short-term sea level fluctuations. Components computed only for El Niño and La Niña years are shown by dotted and dashed lines, and grey lines are the sum of the tide, short-term and seasonal components. The 10 highest sea-level events in the record relative to MHHW are shown and coded to indicate the phase of ENSO at the time of the extreme event.

8.7 Climate Projections

Climate projections have been derived from up to 18 global climate models from the CMIP3 database, for up to three emissions scenarios (B1 (low), A1B (medium) and A2 (high)) and three 20-year periods (centred on 2030, 2055 and 2090, relative to 1990). These models were selected based on their ability to reproduce important features of the current climate (Volume 1, Section 5.2.3) so projections from each of the models are plausible representations of the future climate. This means there is not one single projected future for Nauru, but rather a range of possible futures. The full range of these futures is discussed in the following sections.

These projections do not represent a value specific to any actual location, such as a town in Nauru. Instead, they refer to an average change over the broad geographic region encompassing Nauru and the surrounding ocean (Figure 1.1 shows the regional boundaries). Section 1.7 provides important information about interpreting the climate model projections.

8.7.1 Temperature

Surface air temperature and sea-surface temperature are projected to continue to increase over the course of the 21st century. There is *very high* confidence in this direction of change because:

- Warming is physically consistent with rising greenhouse gas concentrations.
- All CMIP3 models agree on this direction of change.

Almost all of CMIP3 models simulate a slight increase (<1°C) in annual and seasonal mean temperature by 2030, however by 2090 under the A2 (high) emissions scenario temperature increases of greater than 3°C are simulated by the majority of models (Table 8.3). Given the close relationship between surface air temperature and sea-surface temperature, a similar (or slightly weaker) rate of warming is projected for the surface ocean (Figure 8.6). There is *moderate* confidence in this range and distribution of possible futures because:

- There is generally close agreement between modelled and observed temperature trends over the past 50 years in the vicinity of Nauru, although observational records are limited (Figure 8.6).
- In simulations of the current climate, almost all CMIP3 models have a cold temperature bias in the vicinity of Nauru (known as the 'cold tongue bias'; Volume 1, Section 5.2.2.1).

Interannual variability in surface air temperature and sea-surface temperature over Nauru is strongly influenced by ENSO in the current climate. As there is no consistency in projections of future ENSO activity (Volume 1, Section 6.4.1) it is not possible to determine whether interannual variability in temperature will change in the future. However, ENSO is expected to continue to be an important source of variability for the region.

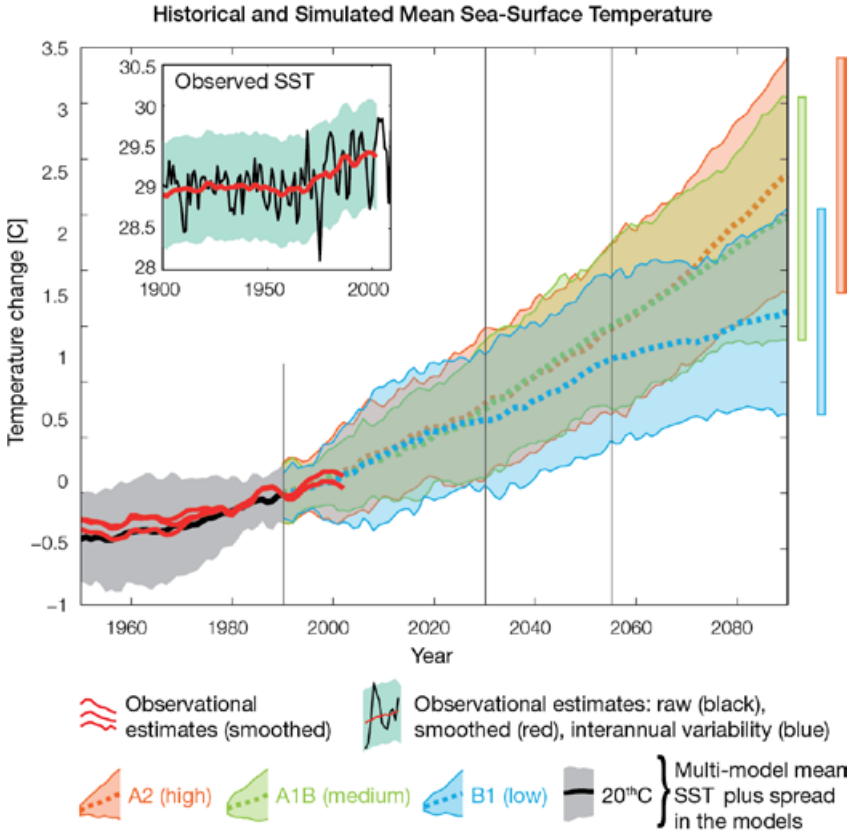

Figure 8.6: Historical climate (from 1950 onwards) and simulated historical and future climate for annual mean sea-surface temperature (SST) in the region surrounding Nauru, for the CMIP3 models. Shading represents approximately 95% of the range of model projections (twice the inter-model standard deviation), while the solid lines represent the smoothed (20-year running average) multi-model mean temperature. Projections are calculated relative to the 1980–1999 period (which is why there is a decline in the inter-model standard deviation around 1990). Observational estimates in the main figure (red lines) are derived from the HadSST2, ERSST and Kaplan Extended SST V2 datasets (Volume 1, Section 2.2.2). Annual average (black) and 20-year running average (red) HadSST2 data is also shown inset.

8.7.2 Rainfall

Wet season (November-April), dry season (May-October) and annual average rainfall are projected to increase over the course of the 21st century. There is *high* confidence in this direction of change because:

- Physical arguments indicate that rainfall will increase in the equatorial Pacific in a warmer climate (IPCC, 2007; Volume 1, Section 6.4.3).
- Almost all of the CMIP3 models agree on this direction of change.

The majority of CMIP3 models simulate an increase (>5%) in annual and seasonal mean rainfall by 2030, with almost all models simulating a large increase (>15%) by 2090 (Table 8.3). There is *low* confidence in this range and distribution of possible futures because:

- In simulations of the current climate, almost all CMIP3 models substantially underestimate present day rainfall in the vicinity of Nauru, in association with the cold tongue bias (Volume 1, Section 5.2.1.2).
- The CMIP3 models are unable to resolve many of the physical processes involved in producing rainfall. As a consequence, they do not simulate rainfall as well as other variables such as temperature (Volume 1, Chapter 5).

Interannual variability in rainfall over Nauru is strongly influenced by ENSO in the current climate (Section 8.5). As there is no consistency in projections of future ENSO activity (Volume 1, Section 6.4.1), it is not possible to determine whether interannual variability in rainfall will change in the future.

8.7.3 Extremes

Temperature

The intensity and frequency of days of extreme heat are projected to increase over the course of the 21st century. There is *very high* confidence in this direction of change because:

- An increase in the intensity and frequency of days of extreme heat is physically consistent with rising greenhouse gas concentrations.
- All CMIP3 models agree on the direction of change for both intensity and frequency.

The majority of CMIP3 models simulate an increase of approximately 1°C in the temperature experienced on the 1-in-20-year hot day by 2055 under the B1 (low) emissions scenario, with an increase of over 2.5°C simulated by the majority of models by 2090 under the A2 (high) emissions scenario (Table 8.3). There is *low* confidence in this range and distribution of possible futures because:

- In simulations of the current climate, the CMIP3 models tend to underestimate the intensity and frequency of days of extreme heat (Volume 1, Section 5.2.4).

Smaller increases in the frequency of days of extreme heat are projected by the CCAM 60 km simulations.

Rainfall

The intensity and frequency of days of extreme rainfall are projected to increase over the course of the 21st century. There is *high* confidence in this direction of change because:

- An increase in the frequency and intensity of extreme rainfall is consistent with larger-scale projections, based on the physical argument that the atmosphere is able to hold more water vapour in a warmer climate (Allen and Ingram, 2002; IPCC, 2007). It is also consistent with physical arguments that rainfall will increase in the deep tropical Pacific in a warmer climate (IPCC, 2007; Volume 1, Section 6.4.3).
- Almost all of the CMIP3 models agree on this direction of change for both intensity and frequency.

The majority of CMIP3 models simulate an increase of at least 15 mm in the amount of rain received on the 1-in-20-year wet day by 2055 under the B1 (low) emissions scenario, with an increase of at least 35 mm simulated by 2090 under the A2 (high) emissions scenario. The majority of models project that the current 1-in-20-year extreme rainfall event will occur, on average, three to four times per 20-year period by 2055 under the B1 (low) emissions scenario and six to seven times per 20-year period by 2090 under the A2 (high) emissions scenario. There is *low* confidence in this range and distribution of possible futures because:

- In simulations of the current climate, the CMIP3 models tend to underestimate the intensity and frequency of extreme rainfall (Volume 1, Section 5.2.4), particularly in the vicinity of Nauru, in association with the cold tongue bias (Volume 1, Section 5.2.1.2).
- The CMIP3 models are unable to resolve many of the physical processes involved in producing extreme rainfall.

Drought

The incidence of drought is projected to decrease over the course of the 21st century. There is *moderate* confidence in this direction of change because:

- A decrease in drought is consistent with projections of increased rainfall (Section 8.7.2).
- The majority of models agree on this direction of change for all drought categories.

The majority of CMIP3 models project that mild drought will occur approximately seven to eight times every 20 years in 2030 under the B1 (low) and A1B (medium) emissions scenarios, decreasing to six to seven times by 2090. For the A2 (high) emissions scenario, a more pronounced decline from eight to nine times every 20 years in 2030 to five to six times by 2090 is projected. The frequency of moderate drought is projected to decline from two to three times every 20 years in 2030 to once to twice every 20 years in 2090 for all emissions scenarios, while severe droughts are expected to decline from once to twice to once every 20 years over the same periods. There is *low* confidence in this range and distribution of possible futures because:

- There is only low confidence in the range of rainfall projections (Section 8.7.2), which directly influences projections of future drought conditions.

8.7.4 Ocean Acidification

The acidification of the ocean will continue to increase over the course of the 21st century. There is *very high* confidence in this projection as the rate of ocean acidification is driven primarily by the increasing oceanic uptake of carbon dioxide, in response to rising atmospheric carbon dioxide concentrations.

Projections from all analysed CMIP3 models indicate that the annual maximum aragonite saturation state will reach values below 3.5 by about 2040 and continue to decline thereafter (Figure 8.7; Table 8.3). There is *moderate* confidence in this range and distribution of possible futures because the projections are based on climate models without an explicit representation of the carbon cycle and with relatively low resolution and known regional biases.

The impact of acidification change on the health of reef ecosystems is likely to be compounded by other stressors including coral bleaching, storm damage and fishing pressure.

8.7.5 Sea Level

Mean sea level is projected to continue to rise over the course of the 21st century. There is *very high* confidence in this direction of change because:

- Sea-level rise is a physically consistent response to increasing ocean and atmospheric temperatures, due to thermal expansion of the water and the melting of glaciers and ice caps.
- Projections arising from all CMIP3 models agree on this direction of change.

The CMIP3 models simulate a rise of between approximately 5–15 cm by 2030, with increases of 20–60 cm indicated by 2090 under the higher emissions scenarios (i.e. A2 (high), A1B (medium); Figure 8.8; Table 8.3). There is *moderate* confidence in this range and distribution of possible futures because:

- There is significant uncertainty surrounding ice-sheet contributions to sea-level rise and a rise larger than projected above cannot be excluded (Meehl et al., 2007b). However, understanding of the processes is currently too limited to provide a best estimate or an upper bound (IPCC, 2007).
- Globally, since the early 1990s, sea level has been rising near the upper end of these projections. During the 21st century, some studies (using semi-empirical models) project faster rates of sea-level rise.

Interannual variability of sea level will lead to periods of lower and higher regional sea levels. In the past, this interannual variability has been about 23 cm (5–95% range, after removal of the seasonal cycle; dashed lines in Figure 8.8 (a)) and it is likely that a similar range will continue through the 21st century. In addition, winds and waves associated with weather phenomena will continue to lead to extreme sea-level events.

In addition to the regional variations in sea level associated with ocean and mass changes, there are ongoing changes in relative sea level associated with changes in surface loading over the last glacial cycle (glacial isostatic adjustment) and local tectonic motions. The glacial isostatic motions are relatively small for the PCCSP region.

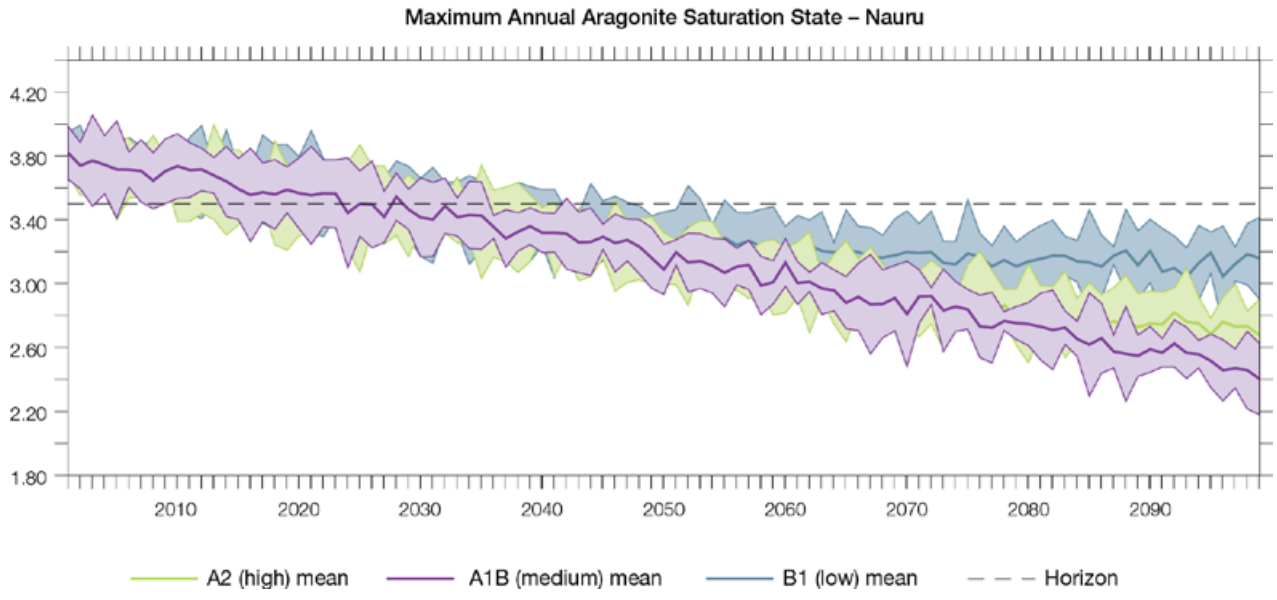

Figure 8.7: Multi-model projections, and their associated uncertainty (shaded area represents two standard deviations), of the maximum annual aragonite saturation state in the sea surface waters of the Nauru region under the different emissions scenarios. The dashed black line represents an aragonite saturation state of 3.5.

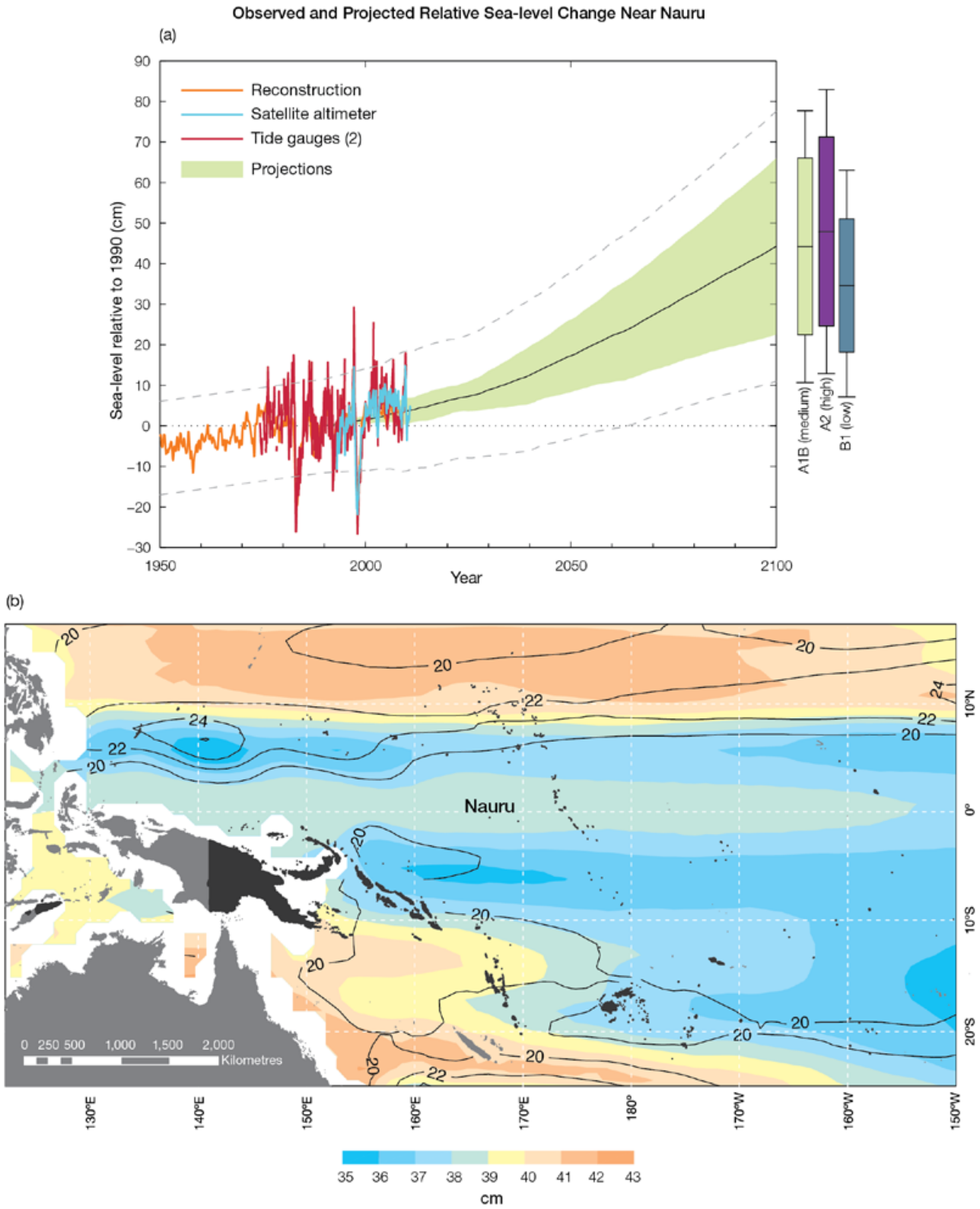

Figure 8.8: Observed and projected relative sea-level change near Nauru. (a) The observed in situ relative sea-level records are indicated in red, with the satellite record (since 1993) in light blue. The gridded sea level at Nauru (since 1950, from Church and White (in press)) is shown in orange. The projections for the A1B (medium) emissions scenario (5–95% uncertainty range) are shown by the green shaded region from 1990–2100. The range of projections for the B1 (low), A1B (medium) and A2 (high) emissions scenarios by 2100 are also shown by the bars on the right. The dashed lines are an estimate of interannual variability in sea level (5–95% range about the long-term trends) and indicate that individual monthly averages of sea level can be above or below longer-term averages. (b) The projections (in cm) for the A1B (medium) emissions scenario in the Nauru region for the average over 2081–2100 relative to 1981–2000 are indicated by the shading, with the estimated uncertainty in the projections indicated by the contours (in cm).

8.7.6 Projections Summary

The projections presented in Section 8.7 are summarised in Table 8.3. For detailed information regarding the various uncertainties associated with the table values, refer to the preceding text in Sections 8.7 and 1.7, in addition to Chapters 5 and 6 in Volume 1. When interpreting the differences between projections for the B1 (low), A1B (medium) and A2 (high) emissions scenarios, it is also important to consider the emissions pathways associated with each scenario (Volume 1, Figure 4.1) and the fact that a slightly different subset of models was available for each (Volume 1, Appendix 1).

Table 8.3: Projected change in the annual and seasonal mean climate for Nauru, under the B1 (low; blue), A1B (medium; green) and A2 (high; purple) emissions scenarios. Projections are given for three 20-year periods centred on 2030 (2020–2039), 2055 (2046–2065) and 2090 (2080–2099), relative to 1990 (1980–1999). Values represent the multi-model mean change ± twice the inter-model standard deviation (representing approximately 95% of the range of model projections), except for sea level where the estimated mean change and the 5–95% range are given (as they are derived directly from the Intergovernmental Panel on Climate Change Fourth Assessment Report values). The confidence (Section 1.7.2) associated with the range and distribution of the projections is also given (indicated by the standard deviation and multi-model mean, respectively). See Volume 1, Appendix 1 for a complete listing of CMIP3 models used to derive these projections.

Variable	Season	2030	2055	2090	Confidence
Surface air temperature (°C)	Annual	+0.7 ± 0.5 +0.8 ± 0.6 +0.8 ± 0.5	+1.3 ± 0.6 +1.6 ± 0.7 +1.6 ± 0.6	+1.7 ± 0.8 +2.6 ± 0.9 +3.0 ± 0.8	Moderate
Maximum temperature (°C)	1-in-20-year event	N/A	+1.0 ± 0.6 +1.4 ± 0.5 +1.5 ± 0.6	+1.3 ± 0.7 +2.2 ± 1.1 +2.7 ± 1.4	Low
Minimum temperature (°C)	1-in-20-year event	N/A	+1.4 ± 2.1 +1.6 ± 3.0 +1.2 ± 2.1	+1.9 ± 2.0 +2.6 ± 2.6 +2.7 ± 2.5	Low
Total rainfall (%)*	Annual	+13 ± 25 +10 ± 24 +11 ± 26	+11 ± 30 +25 ± 33 +25 ± 41	+27 ± 38 +43 ± 64 +45 ± 71	Low
Wet season rainfall (%)*	November-April	+10 ± 27 +10 ± 28 +9 ± 29	+19 ± 27 +21 ± 36 +21 ± 50	+22 ± 34 +35 ± 67 +35 ± 59	Low
Dry season rainfall (%)*	May-October	+16 ± 37 +12 ± 35 +14 ± 34	+30 ± 51 +30 ± 46 +32 ± 49	+35 ± 54 +54 ± 78 +59 ± 97	Low
Sea-surface temperature (°C)	Annual	+0.7 ± 0.6 +0.7 ± 0.6 +0.8 ± 0.7	+1.2 ± 0.7 +1.5 ± 0.7 +1.5 ± 0.8	+1.6 ± 0.9 +2.5 ± 1.1 +2.9 ± 1.1	Moderate
Aragonite saturation state (Ωar)	Annual maximum	+3.5 ± 0.2 +3.4 ± 0.2 +3.4 ± 0.2	+3.2 ± 0.2 +3.1 ± 0.2 +3.1 ± 0.1	+3.1 ± 0.2 +2.7 ± 0.2 +2.5 ± 0.2	Moderate
Mean sea level (cm)	Annual	+8 (4–13) +9 (4–14) +9 (4–14)	+17 (9–25) +20 (10–30) +19 (10–29)	+31 (17–45) +39 (20–57) +40 (21–60)	Moderate

*The MIROC3.2(medres) and MIROC3.2(hires) models were eliminated in calculating the rainfall projections, due to their inability to accurately simulate the South Pacific Convergence Zone and/or the Intertropical Convergence Zone (Volume 1, Section 5.5.1).